JOURNAL OF SOLID STATE CHEMISTRY **121,** 278–290 (1996)
ARTICLE NO. 0039

Crystal/Defect Structures and Phase Stability in Ba Hexaaluminates

Jae-Gwan Park[1] and A. N. Cormack

New York State College of Ceramics at Alfred University, Alfred, New York 14802

Received October 3, 1994; in revised form September 4, 1995; accepted September 7, 1995

Computer atomistic simulation techniques have been used to investigate the crystal chemistry, defect structures, and phase relationships in Ba hexaaluminates. Equilibrated lattice energies for several structural models, proposed to explain the nonstoichiometries of Ba hexaaluminates, have been calculated and suggest that Ba hexaaluminate in the magnetoplumbite structure is unstable compared to nonstoichiometric β-alumina type structures. The lack of superstructure in phase I is explained by the very small difference in lattice energies between the structures in which the defect complex of this phase is differently arranged. Our calculations also suggest that the most appropriate structural model for phase II is one which includes both triple Reidinger defects and barium interstitials inside the spinel blocks from the viewpoint of both energy and crystal symmetry.

1. INTRODUCTION

Hexaaluminates commonly refer to hexagonal poly-aluminates having a structure related to either that of β-alumina (ideal formula $NaAl_{11}O_{17}$) or magnetoplumbite (ideal formula $PbFe_{12}O_{19}$). The two parent structures, β-alumina and magnetoplumbite, are similar, characterized by hexagonal symmetry of space group $P6_3/mmc$. They are composed of spinel structured blocks which are stacked together in a manner relating each block to its adjacent blocks by a mirror plane containing the large cations. Each spinel block consists of four close-packed oxygen layers with trivalent cations in both octahedral and tetrahedral sites. The major difference between the two lies in the structure of mirror plane regions. The unit cell structures of the ideal Na β-alumina and Sr hexaaluminate magnetoplumbite are shown in Fig. 1.

Until the early seventies, Ba hexaaluminate was assigned the magnetoplumbite structure with stoichiometry of $BaAl_{12}O_{19}$, like other hexaaluminates of divalent cations, such as Ca, Sr, or Pb (1, 2). However, several investigations (3–7) have subsequently revealed that the compound "$BaAl_{12}O_{19}$" does not exist, except as a mixture of two distinct nonstoichiometric phases, referred to as phase I and phase II by Kimura *et al.* (4).

Two X-ray single-crystal structural refinement studies, reported by van Berkel *et al.* (8) and Iyi *et al.* (9), have established that the structure of phase I, having structural formula $Ba_{0.75}Al_{11}O_{17.25}$, is of β-alumina type. The defect mechanisms for nonstoichiometry in this compound are very similar to those of cation-excess β-alumina. Recently, Ba hexaaluminate phase I of lower barium content ($Ba_{0.68}Al_{11}O_{17.18}$), having a short-range order in the form of microdomains, was reported (10). On the other hand, although many studies (5–9, 11–15) using X-ray diffractometry, electron microscopy, or EPR spectroscopy, have been devoted to the structure of phase II, having structural model formula $Ba_{2.33}Al_{21.33}O_{34.33}$, there are several different views on the location of the excess barium ions of this Ba-rich phase with respect to the ideal composition. Structural models have yet to be clarified for this phase.

The crystal structure of a barium lead hexaaluminate phase II, reported by Iyi *et al.* (12), is the only one, providing refined structural parameters. This structure may be characterized by having excess barium ions positioned nearly at the centers of the spinel blocks and triple Reidinger defects located around a barium vacancy in the interspinel region. However, by applying a valence sum analysis to the central spinel-block barium site with the Ba–O distances reported by Iyi *et al.* (12), Wagner and O'Keeffe (14) concluded that the excess barium ions are probably not at these central spinel-block sites. Moreover, through a comparison of calculated and experimental high-resolution electron microscopic images they proposed a different structural model for Ba hexagallate of phase II type, which is possibly isostructural with Ba hexaaluminate phase II. In that model, the excess barium ions are positioned midway between the spinel-block centers and alternating mirror planes. On the other hand, the structural model proposed by Zandbergen *et al.* (11) for Ba hexagal-

[1] To whom correspondence should be addressed. Present address: Division of Ceramics, Korea Institute of Science and Technology, P.O. Box 131, Cheongryang, Seoul 130-650, Korea.

0022-4596/96 $18.00

late or hexaaluminate phase II, in which the excess barium ions are accommodated in the mirror planes, also seems to have reasonable defect mechanisms. It was recently suggested from an EPR study by Gbehi *et al.* (15), however, that the structural mechanisms including Ba-rich mirror planes are improbable.

Because of this variety of opinions, in this paper, we aim to elucidate further the crystal chemistry and defect structures in Ba hexaaluminates phase I and phase II and to discover the fundamental reason for the nonexistence of Ba magnetoplumbite, $BaAl_{12}O_{19}$. Our method is to calculate the lattice energies and equilibrated structures for structural models using atomistic simulation techniques described in the next section.

2. SIMULATION TECHNIQUES

2.1. Potential Models

The simulations in this study are based on the Born model description of solid, which treats the solid as a collection of point ions with short-range forces acting between them. The approach has enjoyed a wide range of success, but it has been found that the reliability of the simulations depends on the validity of the potential model used in the calculations.

The short-range potentials are usually described by a simple analytical Buckingham function,

$$V_{ij}(r_{ij}) = A_{ij}\exp(-r_{ij}/\rho_{ij}) - C_{ij}r_{ij}^{-6}, \qquad [1]$$

where r_{ij} is the distance between the ions i and j.

The polarizability of individual ions is included through the shell model originally developed by Dick and Overhauser (16), in which the outer valence electron cloud of the ion is simulated by a massless shell of charge Y and the nucleus and inner electrons by a core of charge X. The total charge of the ion is, thus, $X + Y$, which equals the oxidation state of the ion. The interaction between the core and shell of any ion is harmonic with a spring constant k and is given by

$$V_i(r_i) = 1/2\, k_i\, d_i^2, \qquad [2]$$

where d_i is the relative displacement of the core and shell of ion i.

For the shell model, the value of the free-ion electronic polarizability is given by

$$\alpha_i = Y_i^2/k_i. \qquad [3]$$

The potential parameters A, ρ, and C in Eq. [1], the shell charge Y, and spring constant k, associated with the shell-model description of polarizability, need to be determined for each interaction and ion type in the crystal. In the present study, they were taken from the compilation of Lewis and Catlow (17) and are listed in Table 1. The O–O interaction was taken from the earlier work of Catlow (18). The viability of these potential models for hexaaluminates was fully discussed in one of our recent works (19). It was shown that the potential models, with a consideration of the effect of coordination number of the short range potential only within the spinel blocks, yielded reasonable simulation results for the thermodynamic stabilities of alkaline earth hexaaluminates, as well as for reproducing the complex crystal structure of strontium magnetoplumbite.

TABLE 1
Interatomic Potential Parameters Used in This Study

Interaction	A (eV)	ρ (Å)	C (eV Å^{-6})
(a) Short range parameters for potential form $V(r) = A\exp(-r/\rho) - Cr^{-6}$			
Sr–O	1400.00	0.35000	0.000
Ba–O	931.70	0.39490	0.000
Al–O	1474.40 [1334.31][a]	0.30059	0.000
O–O	22764.20	0.14910	17.890

(b) Shell parameters

Interaction	Shell charge	Spring constant
Sr(core)–Sr(shell)	1.330	21.53
Ba(core)–Ba(shell)	1.460	14.78
Al(core)–Al(shell)	3.000	99999.99
O(core)–O(shell)	−2.207	27.29

[a] Value of A in this bracket is appropriate for Al ions in a tetrahedral site.

2.2. Lattice Energy Minimization

The lattice energy is the binding or cohesive energy of the perfect crystal and is usually defined as the energy that must be released to the crystal to separate its component ions into free ions at rest at infinite separation. It is of central importance in treating thermochemical properties of solids and in assessing the relative stabilities of different structures. Moreover, its derivatives with respect to elastic strain and displacement are related to dielectric, piezoelectric and elastic constants, and phonon dispersion curves.

The lattice energy is calculated in the Born model of the solid by the relation

$$U = 1/2\, \Sigma\Sigma\, V_{ij}, \qquad [4]$$

where the total pairwise interatomic potential, V_{ij}, is given by

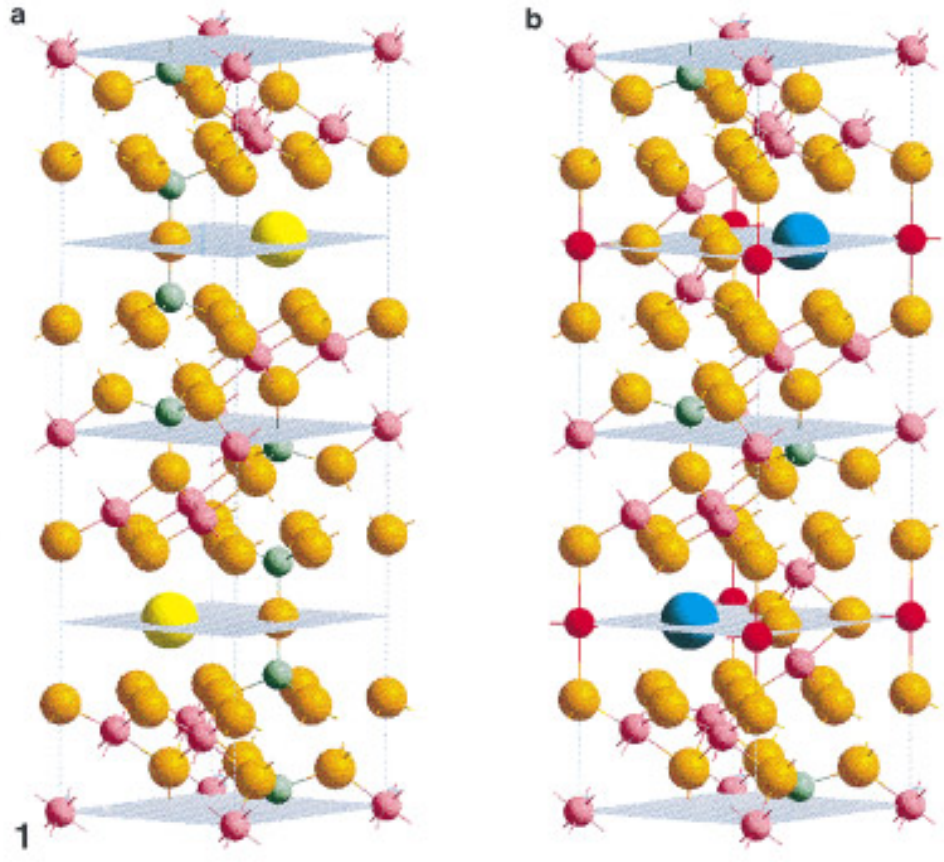
a
b
1

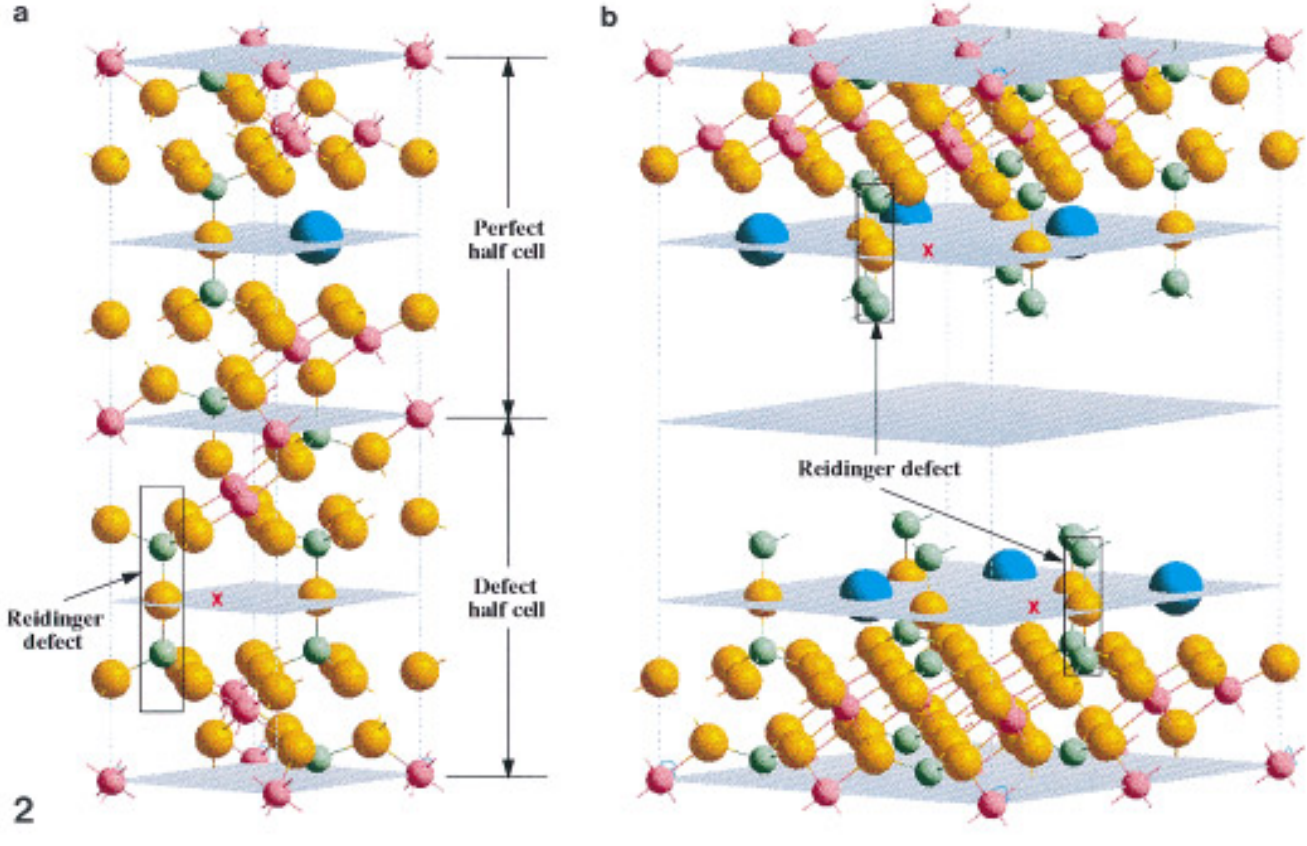
a
b
Perfect
half cell
Defect
half cell
Reidinger
defect
Reidinger defect
2

$$V_{ij}(r_{ij}) = q_i q_j / r_{ij} + A_{ij} \exp(-r_{ij}/\rho_{ij}) - C_{ij} r_{ij}^{-6}, \qquad [5]$$

with the first term representing the Coulombic interactions between species *i* and *j*, and the last two the non-Coulombic short-range contributions discussed above. The lattice energy is thus calculated exactly, and the only limitations in the procedure arise from a lack of precise knowledge of the interatomic potentials.

The lattice energy is minimized through a second derivative Newton-like procedure, coded into METAPOCS (20). Calculation of the equilibrium atomic configuration involves adjusting the coordinates until the internal basis strains (i.e., the net forces acting on a species) are totally removed. For complete structural equilibration (what is generally termed a ''constant pressure condition''), the lattice vectors are also relaxed, using elasticity theory. From the bulk lattice strains obtained from the derivatives of the lattice energy, a new set of basis vectors may be defined. This new lattice vector matrix can thus be expressed directly in terms of the original basis vectors and the bulk lattice strains. The atomic coordinates are then reequilibrated with the new lattice vectors and the procedure repeated until the bulk lattice strains are completely eliminated. Details of the procedure have been outlined by Cormack (21).

The lattice energy calculation is a static lattice calculation. That is to say, no explicit temperature effects are included; the results refer to 0 K calculations of internal energy. However, it has been shown by Gillan (22) that this is often a good approximation to enthalpies at higher temperatures, since the change in internal energy as the lattice expands is to first order equal to the difference between the enthalpy (which is measured) and the 0 K internal energy. The basis for comparison of our calculated results with experiment lies partly in this observation but also in the fact that differences in nonconfigurational entropy between structures which have very similar atomic arrangements are expected to be extremely small, especially at room temperature. This encourages us to ignore entropic effects in structural stability comparison.

3. STRUCTURAL MODELS FOR SIMULATION

Several input structural models based on experimentally proposed structures are set up for simulation. The β-alumina structure used, as a reference point for the input models, is an idealized modification of the structure of sodium β-alumina reported by Peters *et al.* (23): the large cation and the oxygen in the mirror plane are assumed to be only at the 2*d* Beevers–Ross (BR) site and at the 2*c* site, respectively.

3.1. Ideal Ba Magnetoplumbite [*Ba-MP*], $BaAl_{12}O_{19}$

The first structural model of Ba hexaaluminates is the ideal Ba magnetoplumbite, having the crystal structure of Sr magnetoplumbite, $SrAl_{12}O_{19}$. The input structural model Ba-MP is generated from the Sr magnetoplumbite structure reported by Lindop *et al.* (24) with the substitution of barium for strontium.

3.2. Ba Hexaaluminate Phase I [*Ba-*β*(I)*], $Ba_{0.75}Al_{11}O_{17.25}$

The crystal structure of phase I is well characterized in the two independent studies by van Berkel *et al.* (8) and Iyi *et al.* (9). In their proposed structural model, there are two kinds of half unit cell which contain a mirror plane and a spinel block: one is a perfect half cell having the ideal β-alumina structure, and the other is a defect half cell containing a barium vacancy and a so-called Reidinger defect, a string of point defects running parallel to the *c* axis: V_{Al}-Al_i-O_i-Al_i-V_{Al}, in Kroger–Vink notation (Fig. 2a). This defect complex is found in nonstoichiometric cation-excess β-aluminas. Essentially, the oxygen interstitial is a compensating defect, situated at a mid-oxygen (mO) site in the mirror plane and stabilized by the displacement of aluminum ions from lattice sites in the spinel blocks into the mirror plane region. The ratio of the perfect to the defect cell is three to one, for charge neutrality reasons. Furthermore, a random distribution of the two kinds of half unit cell was inferred from the lack of superstructure reflections.

A number of input structural models for simulation of Ba hexaaluminate phase I are generated from the proposed structure assuming that this phase has a superstructure based on a $2a \times 2a \times c$ quadruple cell of β-alumina. The superstructure cell, the formula of which is $Ba_6Al_{88}O_{138}$, contains eight half unit cells of β-alumina, among which six are the perfect and two are the defect cells. The supercell may have various structures according to the distribution of the defects, barium vacancy, and the Reidinger

FIG. 1. Unit cells of the two parent structures of hexaaluminates, (a) Na β-alumina and (b) Sr aluminate magnetoplumbite. (Yellow = Na, blue = Sr, orange = O, pink = Al [6], green = Al [4], and red = Al [5]).

FIG. 2. (a) Structural units in the model for Ba hexaaluminate phase I and (b) the input quadruple supercell of the model Ba-β(I)-b1, containing six perfect and two defect half cells. Atoms in the inner spinel block are not shown in part b for simplicity. In the other models for this phase I, the Ba vacancies and the Reidinger defects are differently distributed within this supercell. (Blue = Ba, others are the same as in Fig. 1. The x indicates Ba vacancy.)

defect. The two barium vacancies may be distributed in three crystallographically distinct ways within the supercell: (a) they are located on a same mirror plane, (b) one vacancy lies on a mirror plane and the other on the other mirror plane in a same basic cell, and (c) they are on different mirror planes and not in a same basic cell. The Reidinger defect may have three different positions around a barium vacancy (recall that there are three mO sites around the vacancy). Consequently, 10 crystallographically distinct structures are possible in the supercell, four structures from the first distribution of the barium vacancies, another four from the second, and two from the third. Therefore, ten input structural models, the Ba-β(I) series, are investigated for this phase. The "Ba-β(I)-*b*1," for example, refers to one of the four models having the second barium vacancy distribution *b*. (See Fig. 2b for its detailed structure.)

3.3. Ba Hexaaluminate Phase II [*Ba-β(II)*], $Ba_{2.33}Al_{21.33}O_{34.33}$

For Ba hexaaluminate phase II, the diffraction evidence suggests a $\sqrt{3}a \times \sqrt{3}a \times c$ supercell, and at least three different structural models have been proposed. The model proposed by Zandbergen *et al.* (11) may be described as follows: two of the three bridging Al_2O groups in a mirror plane region between spinel blocks in a $\sqrt{3}a \times \sqrt{3}a \times c$ supercell of β-alumina are replaced by one barium and one bridging Al_2O_3 group. This Al_2O_3 group consists of two face-sharing octahedra, as found in the magnetoplumbite structure. By the replacement, charge neutrality is obtained and the formula of the supercell becomes $Ba_7Al_{64}O_{103}$. In addition, it is suggested that the aluminum ions on the three-fold axis, at which the substitution of Ba for Al_2O has taken place, shift toward the mirror plane moving from tetrahedral to octahedral sites.

The input structural model Ba-β(II)-Z1 is generated in the triple β-alumina supercell, in consideration of the replacement in the mirror plane region and the displacement of aluminum ions described in the model of Zandbergen *et al.* (11). In a variant of this model, Ba-β(II)-Z2, the replacement in the mirror plane region is considered but the initial displacement is not.

In the structural model of phase II proposed by Iyi *et al.* (12, 13), there are two kinds of basic cell: one is a perfect cell having the ideal β-alumina structure, and the other is a defect cell which contains the excess barium of this phase. There are two main features to this defect cell. One is the presence of three Reidinger defects located around a barium vacancy in a mirror plane. Three interstitial oxygen ions, each of which is stabilized by the two aluminum ions shifting from the neighboring spinel blocks, are positioned at mO sites around the barium vacancy. Therefore, in the defect cell, there are three aluminum vacancies in each spinel block according to the formation of the triple Reidinger defects. The other feature is the existence of barium interstitials within the spinel blocks. This interstitial barium site requires removal of an oxygen ion and an aluminum ion in the spinel block in addition to the three aluminum vacancies, becoming coordinated by twelve oxygens. The oxygen ion, which was coordinated to the three aluminum vacancies simultaneously, is removed together with the aluminum ion connected directly to it. Consequently, the 12-coordinated spinel block barium site requires removal of an OAl_4 tetrahedron in the spinel block. Charge neutrality requires a ratio of two perfect cells to one defect cell with an ordered distribution to give a $\sqrt{3}a \times \sqrt{3}a \times c$ supercell structure. The chemical formula of the supercell becomes $Ba_7Al_{64}O_{103}$.

For considering all the defects described in the model of Iyi *et al.* (12), the input structural model for simulation, Ba-β(II)-I, is generated in the triple β-alumina cell. In this input structure, the oxygen interstitials of the triple Reidinger defect are at mO sites around the barium vacancy in the mirror plane, and the barium interstitials in the spinel blocks are at the centers of the 12-coordinated oxygen polyhedra.

The structural model of phase II suggested by Wagner and O'Keeffe (14) is also based on the $\sqrt{3}a \times \sqrt{3}a \times c$ triple cell of β-alumina and can be described as follows: (i) the two oxygen ions directly above and below one of the three anti-Beevers–Ross (aBR) sites on a mirror plane in the triple cell are replaced by barium ions, (ii) the six aluminum positions which become coordinated to the excess barium ions are vacated, (iii) on the mirror plane directly above and below which the excess barium ions are located, one of the three barium ions at the Beevers–Ross (BR) sites in the triple cell is replaced by a bridging Al_2O_3 group consisting of two face-sharing octahedra, (iv) two additional aluminum ions are introduced into the mirror plane near the Al_2O_3 group, and (v) the resulting supercell has formula $Ba_7Al_{64}O_{103}$, exactly the same as other models.

Since the locations of the two aluminum ions on the mirror plane are not specified in this model, several input structural models, the Ba-β(II)-W series, having different locations of the two aluminum ions, are generated in the triple ideal β-alumina cell. There are three fivefold coordinated (trigonal bipyramidal) sites and four eightfold coordinated sites, which may be available for the two aluminum ions, on the mirror plane near the Al_2O_3 group in the input supercell, when all the defects whose positions are specified are considered. There are also several different possible aluminum sites on the mirror plane in the structure. Among the various possible aluminum sites, two were chosen for the input aluminum sites in each structural model. For simplicity, details of the positions of the two aluminum ions in each model are not given here. It is noteworthy

TABLE 2
Experimental and Simulated Structural Parameters in Sr and Ba Magnetoplumbites

Data from experiment (24)			Data from calculation					
Sr magnetoplumbite			Sr–MP			Ba–MP		
a = 5.562 Å c = 21.972 Å $P6_3/mmc$			a = 5.6581 Å c = 21.6676 Å $P6_3/mmc$			a = 5.6793 Å c = 21.8927 Å $P6_3mc$		
Atom	Site	Coordinates	Atom	Site	Coordinates	Atom	Site	Coordinates
Sr	2*d*	*x* 0.6667 *z* 0.2500	Sr	2*d*	*x* 0.6667 *z* 0.2500	Ba	2*b*	*x* 0.6667 *z* 0.2518
Al(2)	2*b*	*x* 0.0000 *z* 0.2500	Al(2)	2*b*	*x* 0.0000 *z* 0.2500	Al(2)	2*a*	*x* 0.0000 *z* 0.2424
Al(5)	4*f*	*x* 0.3333 *z* 0.1903	Al(5)	4*f*	*x* 0.3333 *z* 0.1883	Al(5)	2*b*	*x* 0.3333 *z* 0.1871
						Al(5)′	2*b*	*x* 0.3333 *z* 0.3127
O(3)	6*h*	*x* 0.1822 *z* 0.2500	O(3)	6*h*	*x* 0.1829 *z* 0.2500	O(3)	6*c*	*x* 0.1827 *z* 0.2487

that the highest crystal symmetry of the supercell possible in this structural model Ba-β(II)-W is not hexagonal or trigonal but orthorhombic (*Cmm2*), due to the low symmetric arrangement (it can not have a 3 or $\bar{3}$ axis as well as a 6 or $\bar{6}$ axis) of the proposed defects.

4. RESULTS AND DISCUSSION

4.1. Equilibrated Structures

4.1.1. Ba magnetoplumbite, Ba-MP. The equilibrium positional parameters for atoms of the model Ba-MP, given in Table 2, are compared with the simulation result (Sr-MP) and the experimental X-ray structure of Sr magnetoplumbite. (For simplicity, only parameters for the atoms in the interspinel region are listed.) From Table 2, we can see that the X-ray and the equilibrated structures of Sr magnetoplumbite are in good agreement concerning both crystal symmetry and atomic coordinates. The success of these calculations in correctly reproducing the complex magnetoplumbite crystal structure provided partial support for the viability of the potential models used in this study, allowing us to continue the calculations for other models.

A noteworthy feature in the equilibrated structure of Ba-MP is the lowering of the crystal symmetry to the space group $P6_3mc$ from the $P6_3/mmc$ of the magnetoplumbite structure. The mirror plane symmetry perpendicular to the *c* axis is lost. The aluminum, barium, and oxygen ions in the mirror plane of the magnetoplumbite structure are no longer in a plane but in a slab in the equilibrated structure of Ba-MP. This result is due to the fact that the large size (that is, the large short-range repulsive interaction) of the barium ion does not allow the coplanar arrangement of those ions, in conjunction with the atomic arrangement in the spinel blocks. This decrease of symmetry is an indication of the structural instability of the magnetoplumbite-structured $BaAl_{12}O_{19}$; the ideal MP structure is not suitable with Ba, as opposed to Sr (or Ca). In spite of the structural distortion, this Ba-MP is still energetically unstable compared to a mixture of the two nonstoichiometric β-alumina-type phases, as will be described later: the lowering of symmetry is not sufficient to maintain the MP-type stoichiometry and structure for Ba against decompo sition into the two nonstoichiometric β-alumina-type phases.

4.1.2. Ba hexaaluminate phase I, Ba-β(I). The basic β-alumina structure is maintained in all of the equilibrated supercell structures, although there is a small amount of lattice relaxation around the barium vacancies and the Reidinger defects. However, the equilibrated supercells do not have exact hexagonal structures but pseudo-hexagonal structures. Though the mirror plane symmetry perpendicular to the hexagonal *c* axis is not destroyed, the interaxial angles γ deviate slightly from 120°. The exact symmetries of the equilibrated structures are monoclinic or orthorhombic. However, these pseudo-hexagonal (monoclinic or orthorhombic) symmetries seem to result from the assumption of a superstructure which is lacking in the real system, rather than being inherent properties. If the random distribution of the defect half cells throughout the crystal is taken into ac-

count (by, for example, using a bigger supercell in the calculations), the structure should have an exact hexagonal symmetry.

4.1.3. Ba hexaaluminate phase II, Ba-β(II). The equilibrated supercell structures of the models Ba-β(II)-Z1 and Ba-β(II)-Z2 were found to have the space group symmetry $P\bar{6}$ (as do the average subcell structures).

A result worthy of notice in the simulation of both models is that a relaxation of aluminum ions in the spinel blocks, which is similar to the displacement suggested by Zandbergen *et al.* (11), occurred naturally in the equilibrated structures. The naturally relaxing species, however, is not the aluminum ion (Al(a)), located on a triad at which the substitution of an Al_2O group by a Ba takes place, suggested by them, but the ion (Al(b)) located on a different triad at which the substitution of an Al_2O group by an Al_2O_3 group takes place. In other words, the Al(b) shifts naturally towards the substituting Al_2O_3 group, moving from tetrahedral to octahedral sites, regardless of the former Al(a) is or is not initially displaced. (Recall that the displacement of the Al(a) is included in the input model of Ba-β(II)-Z1, but not in that of Ba-β(II)-Z2.) Although the relaxation of the Al(a) did not occur naturally, the structure including it yielded a slightly lower lattice energy than that without it, suggesting the relaxation is also energetically favorable. (The lattice energies are given later.) Therefore, the relaxing species should include both of the two aluminum ions, Al(a) and Al(b), so far as the structural model of Zandbergen *et al.* (11) is concerned. These relaxations of aluminum ions within the spinel blocks toward the defect mirror planes relieve the electrostatic potential imposed on the spinel blocks by the two neighboring interspinel layers; one, the perfect layer, and the other, the defect layer, have effective charges of +3 and −3, respectively, in the supercell, compared to the ideal triple cell of Na β-alumina. Note that the Al_2O_3 group and the Ba ion, substituting the Al_2O groups in the defect interspinel layer, have effective charges of −4 and −2, respectively. One noteworthy aspect of the relaxations of aluminum ions is that due to the repulsive Coulombic potential between the Al(b) and the aluminum ion of the Al_2O_3 group, the Al(b) can not be centered on the octahedral site, but is greatly off-centered, forming a severely distorted octahedron. On the other hand, in the case of Al(a), the degree of off-centering is not so great, since the potential between the Al(a) and the Ba is less repulsive (due to the longer distance and lower charges) than the preceding interaction. This structural information may be a moot point, however, because this model Ba-β(II)-Z1 is not predicted to be the most energetically favored.

The equilibrated structure for the second model of the phase II, Ba-β(II)-I (that of Iyi *et al.*), is shown in Fig. 3, in which the ideal β-alumina triple cell is also given for comparison. The equilibrated supercell of the model Ba-β(II)-I has the space group symmetry $P\bar{6}2m$, whilst the average subcell (β-alumina basic cell) has the symmetry $P\bar{6}m2$. These space group symmetries are consistent with those revealed by Iyi *et al.* through x-ray diffraction (12) and CBED/HREM (convergent beam electron diffraction/high-resolution electron microscopy) (13) studies, respectively. In Table 3, the equilibrated cationic positions in the average subcell of symmetry $P\bar{6}m2$ are compared with the experimental parameters reported by Iyi *et al.* (12). The equilibrated structural parameters of all ions in the supercell of symmetry $P\bar{6}2m$ are given in Table 4. We can see a good agreement between our calculated coordinates and their experimental ones in Table 3, especially given both the complexity of this structure and the chemical difference between the simulation and the experiment (20% of Ba ions were substituted by Pb ions in the experiment). These structural compatibilities of symmetry and coordinates between simulation and experiment are strong evidence for this structural model. The Ba–O bond distances in the equilibrated structure are given in Table 5.

In this structure, it can be regarded that the Coulombic strain between the perfect mirror plane and the defect mirror plane, whose effective charges are +3 and −5, respectively, relative to the ideal β-alumina triple cell, is relieved mainly by the relaxation of aluminum ions (Al(8)) from spinel-block octahedral sites to interspinel-layer tetrahedral sites. These form Al_2O bridges of the Reidinger defects with the charge-compensating interstitial oxygens (O(11)) in the defect mirror plane. The compensating oxygens (O(11)) are relaxed from the input mO sites, due to the repulsion between them. The oxygens (O(9)) on the defect mirror plane, which were positioned at the ideal oxygen sites in the input structure, are also relaxed. Therefore, the Al_2O bridges connecting spinel blocks in the defect mirror plane region are no longer linear.

It may be generally considered that the spinel block structure is so stable that the central spinel-block barium interstitials are not likely to exist. However, a barium ion seems to be incorporated without difficulty into the spinel block matrix, given not only the removal of an oxygen and an adjacent aluminum ion in the spinel block (see Section 3.3) but also the relaxation of the three aluminum ions (Al(8)) to the mirror plane region, forming the triple Reidinger defects. The incorporation is confirmed indirectly by the fact that the coordination polyhedra of the remaining aluminum ions in the equilibrated spinel block matrix show little distortion, in spite of the structural and chemical disturbance by the defects. The equilibrium position of the barium ion (Ba(3)) at the 12-coordinated central spine-block site is slightly off from the center of the spinel block. The agreement between the coordinates of this site from simulation and experiment may also be evidence of this unusual incorporation.

Wagner and O'Keeffe (14) raised an objection, however,

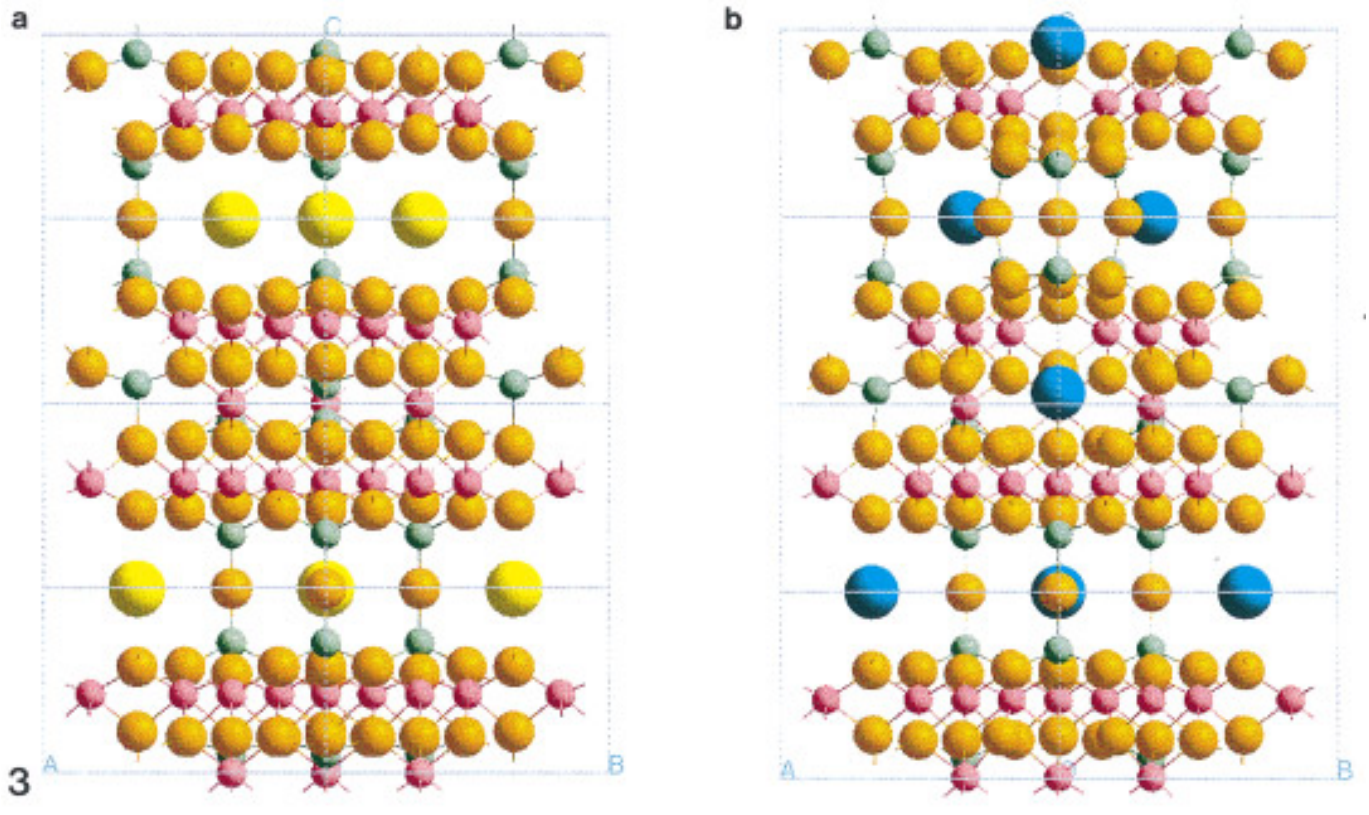

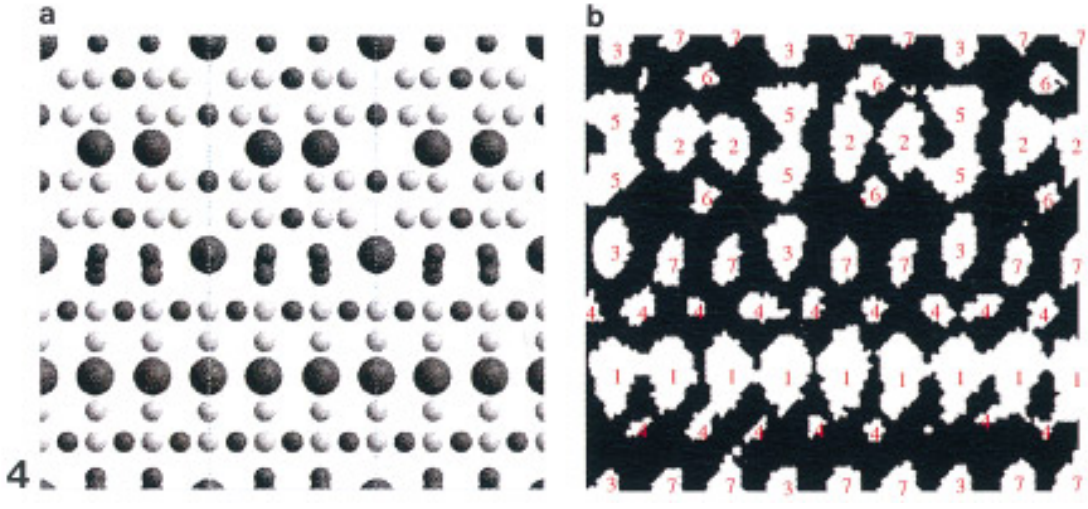

FIG. 3. The [110] directional views of (a) the ideal Na β-alumina triple cell and (b) the equilibrated supercell of Ba-β(II)-I. The defects in the latter structure are accommodated by only very localized lattice relaxation. (Color assignments are the same as in Fig. 2.)

FIG. 4. (a) A projection of a barium hexagallate structure, assumed to have the equilibrated structure of Ba-β(II)-I, on the (110) plane of the supercell, in which the sizes of the atoms are proportional to atomic numbers. Oxygens are not shown. The smaller black atoms represent the overlapping atoms. (b) The experimental HREM image of barium hexagallate taken along the [110] direction of the supercell (scan-copied from reference (14)).

TABLE 3
Comparison between Simulated and Experimental Positional Parameters in the Average Basic Cell of Ba-β(II)-I

Data from calculation					Data from x-ray structure (12)			
a = 5.7062 Å c = 22.9701 Å Space group: $P\bar{6}m2$					a = 5.6003(5) Å c = 22.922(2) Å Space group: $P\bar{6}m2$			
Atom	Site	#/cell	Coordinate	Difference	Coordinate	#/cell	Site	Atom
Ba(1)	1*e*	2/3	*x* 0.6667	−0.0103	*x* 0.6770	0.685	3*j*	Ba(1)
			z 0.0000	0.0000	*z* 0.0000			
Ba(2)	3*k*	1	*x* 0.3369	0.0167	*x* 0.3202	1.002	3*k*	Ba(2)
			z 0.5000	0.0000	*z* 0.5000			
Ba(3)	2*i*	2/3	*x* 0.6667	0.0000	*x* 0.6667	0.586	2*i*	Ba(3)
			z 0.2336	0.0134	*z* 0.2202			
Al(1)	12*o*	4	*x* 0.8154	−0.0197	*x* 0.8351	3.96	6*n*	Al(1)
			y 0.6685	0.0017	*y* 0.6702			
			z 0.1530	0.0015	*z* 0.1515			
Al(2)	12*o*	4	*x* 0.1664	0.0004	*x* 0.1660	6	6*n*	Al(2)
			y 0.3313	−0.0007	*y* 0.3320			
			z 0.3563	−0.0010	*z* 0.3573			
Al(2)′	6*n*	2	*x* 0.1695	0.0035				
			z 0.3565	−0.0008				
Al(3)	6*n*	2	*x* 0.3196	−0.0137	*x* 0.3333	2	2*h*	Al(3)
			z 0.2310	0.0008	*z* 0.2302			
Al(4)	2*i*	4/3	*x* 0.6667	0.0000	*x* 0.6667	1.48	2*i*	Al(4)
			z 0.2781	0.0014	*z* 0.2767			
Al(5)	6*n*	2	*x* 0.3041	−0.0043	*x* 0.3084	1.99	6*n*	Al(5)
			z 0.0748	0.0007	*z* 0.0741			
Al(6)	2*i*	4/3	*x* 0.6667	0.0000	*x* 0.6667	2	2*i*	Al(6)
			z 0.4242	−0.0007	*z* 0.4249			
Al(6)′	2*i*	2/3	*x* 0.6667	0.0000				
			z 0.4231	−0.0018				
Al(7)	6*n*	2	*x* 0.0007	0.0007	*x* 0.0000	2	2*g*	Al(7)
			z 0.2528	−0.0004	*z* 0.2532			
Al(8)	6*n*	2	*x* 0.8569	0.0004	*x* 0.8565	1.90	6*n*	Al(8)
			z 0.0710	0.0016	*z* 0.0694			

to this structural model, on the basis of a valence sum analysis (25) for the central spinel-block barium site, using the equation $v_{ij} = \exp\{(R_o - R_{ij})/b\}$ for the bond valences. The calculated bond valence sums of the site for Ba and Pb were 3.11 and 1.95, respectively, with the bond lengths reported by Iyi *et al.* (12) for a barium lead hexaaluminate, Ba(Pb)-β(II).[2] From this result, suggesting that the site was not suited for Ba but for Pb, they proposed that barium hexaaluminate was probably not isostructural with the barium lead hexaaluminate. Furthermore, they proposed a new structural model for Ba hexagallate (or Ba hexaaluminate) having a different spinel block site for the excess barium ions, on the basis of the concept that the barium ions can not be located at the central spinel-block site.

However, judging from the fact that the lattice relaxation around the central spinel-block barium site in the equilibrated structure is substantial, though localized, as can be seen in Fig. 3, it may be very difficult to refine the local structure by X-ray diffraction techniques. This is especially true for the oxygen positions around the barium site. This point seems to be reflected in Iyi *et al.*'s refinement; no distinction was made between the oxygen ions coordinated to Ba and those coordinated to Pb, although these would be expected to occupy different positions. Therefore, it is quite possible that the Ba(3)–O and Pb–O distances

[2] There appears to be an error in the valence sum analysis performed by Wagner and O'Keeffe. They used the Ba(3)–O(3) distance instead of the Ba(3)–O(12) in Table III in Iyi *et al.*'s paper. The Ba(3)–O(3) bonds in the table are not real bonds but the ones originated from the averaging of the two types of unit cells in the structure. Whereas the O(12) ions are found in the defective basic cell containing the Ba (or Pb) ions at its central spinel-block sites, the O(3) ions refer to the perfect basic cell having the ideal β-alumina structure. The corrected values of valence sum would be 2.77 for Ba and 1.74 for Pb with the appropriate Ba–O distances, instead of 3.11 and 1.95, quoted by Wagner and O'Keeffe.

TABLE 4
Positional Parameters of the Equilibrated Supercell Structure of Ba-β(II)-I

Atom	Site	#/cell	x	y	z
Ba(1)	2*c*	2	0.3333	0.6667	0.0000
Ba(2)	3*g*	3	0.3297	0.0000	0.5000
Ba(3)	2*e*	2	0.0000	0.0000	0.2336
Al(1)	12*l*	12	0.3208	0.4928	0.1530
Al(2)	12*l*	12	0.1674	0.3328	0.3563
Al(2)′	6*i*	6	0.4971	0.0000	0.3565
Al(3)	6*i*	6	0.3471	0.0000	0.2310
Al(4)	4*h*	4	0.3333	0.6667	0.2781
Al(5)	6*i*	6	0.3626	0.0000	0.0748
Al(6)	4*h*	4	0.3333	0.6667	0.4242
Al(6)′	2*e*	2	0.0000	0.0000	0.4231
Al(7)	6*i*	6	0.6660	0.0000	0.2528
Al(8)	6*i*	6	0.8098	0.0000	0.0710
O(1)	12*l*	12	0.3555	0.1762	0.2106
O(1)′	6*i*	6	0.5168	0.0000	0.2024
O(2)	12*l*	12	0.6535	0.1560	0.3028
O(2)′	6*i*	6	0.7953	0.0000	0.3073
O(3)	12*l*	12	0.1694	0.5071	0.1108
O(4)	12*l*	12	0.1654	0.4959	0.3958
O(4)′	6*i*	6	0.1719	0.0000	0.3972
O(5)	4*h*	4	0.3333	0.6667	0.1985
O(6)	6*i*	6	0.3346	0.0000	0.3096
O(7)	6*i*	6	0.6661	0.0000	0.1160
O(8)	6*i*	6	0.6613	0.0000	0.3914
O(9)	3*f*	3	0.3947	0.0000	0.0000
O(10)	2*d*	2	0.3333	0.6667	0.5000
O(10)′	1*b*	1	0.0000	0.0000	0.5000
O(11)	3*f*	3	0.7658	0.0000	0.0000
O(12)	6*i*	6	0.1743	0.0000	0.0832

Note. Space group: $P\bar{6}2m$, $a' = 9.8835$ Å, $c' = 22.9701$ Å.

reported in the refined structure are somewhat in error. When we applied the same analysis to the site with the Ba–O distances obtaining in the equilibrated structure, the bond valence sum for Ba was found to be 1.88. This is close to the ideal valence of two for Ba, suggesting that the site in the relaxed hexaaluminate matrix is, indeed, well suited for barium ions as proposed by Iyi *et al*. Consequently, it seems that the refined Ba–O bond distances for the site were underestimated.[3]

Given that the central spinel-block sites are available for barium ions, the high resolution electron microscopic image which was obtained experimentally for barium hexagallate by Wagner and O'Keeffe (14) and became a basis for their model, may in fact be a confirmative (rather than a contradictive) evidence for Iyi *et al*.'s structural model, as discussed by Wagner and O'Keeffe. Figure 4a shows the projection of a barium hexagallate structure, which is assumed to be isostructural with the equilibrated structure of Ba-β(II)-I, onto the (110) plane of the supercell. Figure 4b shows the experimental HREM image of barium hexagallate taken along the [110] direction of the supercell. From a direct comparison between the two figures, the following features of the image may be inferred: (i) all the white spots in the image are in reverse contrast, that is, they represent ''atoms'' in the structure; (ii) among the various Ga atom positions in Fig. 4a, however, only the positions, at which two or three Ga atoms overlap within the thickness of lattice parameter a' of the supercell, appear as white spots in the image (Fig. 4b). Moreover, the white spots numbered 1, 2, and 3 in the image may be attributed to Ba atoms and those numbered 4, 5, 6, and 7 to the overlapping Ga atoms. With these assignments based on the equilibrated structure of Ba-β(II)-I, all of the ''anomalous'' features in the image are successfully explained. Such anomalous features include the periodicities of the spots numbered 3, 5, and 6 and the differences in size and in position between the spots 3 and 7 in the middle of the spinel blocks.

On the other hand, none of the equilibrated supercell structures of the third model for the phase II, Ba-β(II)-W series, has a hexagonal or a trigonal symmetry, as mentioned previously. We found that even the average subcell structures did not have an exact hexagonal symmetry. Moreover, the equilibrated structures in the defect interspinel layer and its neighboring spinel block layers are highly disturbed, compared to the other structural models. This structural disturbance may be ascribed to the antisite defect, the barium ion on oxygen site, in this model. Recall that, in the Ba-β(II)-W series, the excess barium ions are positioned in the oxygen layers directly on either side of an anti-Beevers–Ross site in alternating mirror planes in one of every three subcells. The antisite defect, which is rare in ionic crystals because of the large repulsive Coulombic interaction, also seems to be improbable in hexaaluminate structures. Consequently, from the viewpoint of crystal symmetry, this third structural model is not consistent with any of the structures experimentally suggested for phase II type. The CBED patterns taken along the [001] zone axis for barium hexaaluminate phase II (7) and for barium lead hexaaluminate phase II (13) clearly reveal a 3*m* symmetry. On the contrary, there can be no threefold symmetry even in the input model structures, or in the equilibrated structures of this model.

It is worthy of notice that while all the barium ions in the equilibrated structure of Ba-β(II)-I are coordinated with 9 or 12 oxygens which form a ''stable'' polyhedron of high symmetry, the barium ions, which are not on the perfect mirror planes in the equilibrated structures of Ba-β(II)-Z and Ba-β(II)-W series, do not reside in a 9- or 12-

[3] The valence sum for the nominal Pb site with the refined Pb–O distances is calculated to be 2.74 for Pb and 4.36 for Ba. (The Pb–O(12) distance is 4.021 Å.) The Pb ion is overbonded so that the site is unsuitable even for Pb, to say nothing of Ba. Consequently, the refined Ba–O (and Pb–O) distances seem to be in error; they were underestimated.

TABLE 5
Ba–O Bond Distances in the Equilibrated Structure of the Model Ba-β(II)-I (Å)

Bond	Number of bonds	Distance	Site
Ba(1)–O(3)	6	3.005	Perfect mirror plane Ba site
–O(9)	3	3.037	
Ba(2)–O(4)	4	2.900	Defective mirror plane Ba site
–O(4)′	2	2.831	
–O(10)	2	3.312	
–O(10)′	1	3.259	
Ba(3)–O(1)	6	3.088	Central spinel block Ba site
–O(2)′	3	2.638	
–O(12)	3	3.860	

coordinated ''stable'' oxygen polyhedron. For instance, the Ba ion replacing an Al_2O group in Ba-β(II)-Z is coordinated with the only six oxygens in the first oxygen layers of spinel blocks above and below it and is directly connected to the other three Ba ions in the defective mirror plane. This suggests that these ions may be less stable, which is why these structures are less favored energetically.

4.2. Lattice Energies

The equilibrated lattice energies of the models for Ba hexaaluminates and related oxide phases are listed in Table 6. As can be seen from the table, of the ten models for the phase I, the model Ba-β(I)-*b* series, in which both of the two barium vacancies are located in one of the four basic cells of the supercell (that is, the two defect half cells are adjacent to each other in the *c* direction), have slightly lower energies than other models having different distributions of the defect half cells. Within the Ba-β(I)-*b* series, the model Ba-β(I)-*b*1 has the lowest energy. This lowest lattice energy of the model can be explained by the smallest interaction energy between the two Reidinger defects. The defect complexes tend to be separated as far as possible, since the potential between them is repulsive. The model Ba-β(I)-*b*1 has the largest separation between them among the series. However, the small energy differences (below about 0.3 eV per the basic cell) between the models suggest that this structure is not predominant over other structures. In other words, it may be concluded that the small interaction energies between the defect complexes explain the absence of a superstructure in the phase I. Superlattice formation requires an ordering energy, which is lacking in this case.

On the other hand, the lattice energies of the models for the phase II indicate that the structural model Ba-β(II)-I is more stable, by about 2 eV or more per the basic cell, than the other models, Ba-β(II)-Z and Ba-β(II)-W series. Even though the energy difference is about 0.1% of the total lattice energy, it is not insignificant as a reaction enthalpy of a reaction between oxides: Usually, reactions forming a ternary oxide from its constituent binary oxides have their reaction enthalpies on the order of 0.1% of the total lattice energies of the system. The significance of the energy differences between the models may further be emphasized from the fact that the models have almost the same atomic arrangement except that a small portion (about 10%) of the atoms in the system have different configuration. A structural feature pertaining to the stability of Ba-β(II)-I is that the coordination polyhedra of aluminum ions in the relaxed spinel block matrix are less distorted in this model than in the others. The lower lattice energy of Ba-β(II)-I seems also to be related to the stability of the coordination polyhedra of barium ions in the structure discussed above.

Consequently, the mechanism of charge compensation and defect structures proposed for the nonstoichiometry of Ba hexaaluminate phase II by Iyi *et al.* (12, 13) is most likely also from the viewpoint of energy.

Furthermore, with the model formulas, we can write the following reaction equation for the reaction from Ba magnetoplumbite to Ba hexaaluminates phase I and phase II:

$$\underset{\text{Ba-MP}}{Ba_2Al_{24}O_{38}} \rightarrow (1/5.8)\underset{\text{Ba-}\beta\text{(I)}}{Ba_6Al_{88}O_{138}} + (0.8/5.8)\underset{\text{Ba-}\beta\text{(II)}}{Ba_7Al_{64}O_{103}}.$$

The enthalpy of this reaction is calculated to be -1.79 eV with the simulated lattice energies. This negative enthalpy demonstrates that Ba magnetoplumbite of intermediate composition is to be unstable and to decompose to a mixture of the phase I and phase II having β-alumina type structures.

5. CONCLUSIONS

We have examined, by using atomistic computer simulation techniques, a number of defect structures and models proposed by other workers to explain the nonstoichiometries of Ba hexaaluminates. We have found energetically those which are favored and have analyzed the structures in some detail to uncover why this is so.

Our calculations reveal that barium hexaaluminate will not be stable in the magnetoplumbite phase but will form a mixture of the two nonstoichiometric phases with β-alumina type structures, as found experimentally.

For phase I, the small difference in equilibrated lattice energies between the structural models, in which the defect complex is differently arranged, explains the lack of superstructure.

TABLE 6
The Equilibrated Lattice Energies of the Models for Ba Hexaaluminates and Related Phases (Energies in eV per Formula Unit)

Model	Chemical formula		Lattice energy	
	Supercell	Subcell	Supercell	Subcell
Ba–MP		$Ba_2Al_{24}O_{38}$		−1968.08
Sr–MP		$Sr_2Al_{24}O_{38}$		−1975.24
Ba-β(I)-a1	$Ba_6Al_{88}O_{138}$	$Ba_{1.5}Al_{22}O_{34.5}$	−7180.21	−1795.05
Ba-β(I)-a2	$Ba_6Al_{88}O_{138}$	$Ba_{1.5}Al_{22}O_{34.5}$	−7178.88	−1794.72
Ba-β(I)-a3	$Ba_6Al_{88}O_{138}$	$Ba_{1.5}Al_{22}O_{34.5}$	−7178.51	−1794.63
Ba-β(I)-a4	$Ba_6Al_{88}O_{138}$	$Ba_{1.5}Al_{22}O_{34.5}$	−7175.89	−1793.97
Ba-β(I)-b1	$Ba_6Al_{88}O_{138}$	$Ba_{1.5}Al_{22}O_{34.5}$	−7182.26	−1795.57
Ba-β(I)-b2	$Ba_6Al_{88}O_{138}$	$Ba_{1.5}Al_{22}O_{34.5}$	−7181.20	−1795.30
Ba-β(I)-b3	$Ba_6Al_{88}O_{138}$	$Ba_{1.5}Al_{22}O_{34.5}$	−7181.19	−1795.30
Ba-β(I)-b4	$Ba_6Al_{88}O_{138}$	$Ba_{1.5}Al_{22}O_{34.5}$	−7181.15	−1795.29
Ba-β(I)-c1	$Ba_6Al_{88}O_{138}$	$Ba_{1.5}Al_{22}O_{34.5}$	−7180.64	−1795.16
Ba-β(I)-c2	$Ba_6Al_{88}O_{138}$	$Ba_{1.5}Al_{22}O_{34.5}$	−7180.11	−1795.03
Ba-β(II)-I	$Ba_7Al_{64}O_{103}$	$Ba_{2.33}Al_{21.33}O_{34.33}$	−5303.74	−1767.91
Ba-β(II)-Z1	$Ba_7Al_{64}O_{103}$	$Ba_{2.33}Al_{21.33}O_{34.33}$	−5297.87	−1765.96
Ba-β(II)-Z2	$Ba_7Al_{64}O_{103}$	$Ba_{2.33}Al_{21.33}O_{34.33}$	−5296.38	−1765.46
Ba-β(II)-W1	$Ba_7Al_{64}O_{103}$	$Ba_{2.33}Al_{21.33}O_{34.33}$	−5295.92	−1765.31
Ba-β(II)-W2	$Ba_7Al_{64}O_{103}$	$Ba_{2.33}Al_{21.33}O_{34.33}$	−5292.91	−1764.30
Ba-β(II)-W3	$Ba_7Al_{64}O_{103}$	$Ba_{2.33}Al_{21.33}O_{34.33}$	−5294.36	−1764.79
Ba-β(II)-W4	$Ba_7Al_{64}O_{103}$	$Ba_{2.33}Al_{21.33}O_{34.33}$	−5296.86	−1765.62
Ba-β(II)-W5	$Ba_7Al_{64}O_{103}$	$Ba_{2.33}Al_{21.33}O_{34.33}$	−5296.86	−1765.62
Ba-β(II)-W6	$Ba_7Al_{64}O_{103}$	$Ba_{2.33}Al_{21.33}O_{34.33}$	−5295.55	−1765.18
Aluminum oxide		Al_2O_3		−158.78
Barium oxide		BaO		−31.31
Strontium oxide		SrO		−33.75

For phase II, our calculations clearly show that, of the various structural models proposed experimentally, that of Iyi *et al.* (12, 13), which may be characterized by the triple Reidinger defects and a barium interstitial in the central spinel block, is most likely. This model is equilibrated to a structure having a crystal symmetry consistent with experiments and has the lowest lattice energy. However, the refined X-ray structural parameters, at least, for the oxygens coordinating the central spinel-block large cation site, were seen to be somewhat in error, the Ba–O bond distances at the site being underestimated.

The feasibility of Iyi *et al.*'s description for phase II is also indicated by some detailed structural features pertaining to the central spinel-block site; the incorporation of Ba into the spinel-block site produces a relaxation of the surrounding oxygen ions without distorting severely the coordination polyhedra of the surrounding cations in the spinel block matrices and the valence sum for Ba on the site in the equilibrated structure yields an appropriate value.

Other structural models, containing the excess Ba ions in the mirror plane or in the first spinel-block oxygen layer, are found to be unfavorable from the viewpoint of energy (and/or crystal symmetry), compared to Iyi *et al.*'s model containing the Ba ions at the central spinel blocks.

ACKNOWLEDGMENTS

The U.S. Department of Energy, Office of Basic Energy Sciences is thanked for financial support under Grant DE-FG02-91ER45451. Some of the calculations reported here were performed at the Cornell Theory Center, which is funded in part by New York State, the National Science Foundation, and IBM corporation.

REFERENCES

1. N. A. Toropov, *Dokl. Akad. Nauk SSSR* **6,** 147 (1935).
2. K. Torkar, H. Krischner, and H. Moser, *Monatsh. Chem.* **96,** 423 (1965).
3. F. Haberey, G. Oehlschlegel, and K. Sahl, *Ber. Dtsch. Keram. Ges.* **54,** 373 (1977).
4. S. Kimura, E. Bannai, and I. Shindo, *Mater. Res. Bull.* **17,** 209 (1982).

5. N. Iyi, S. Takekawa, Y. Bando, and S. Kimura, *J. Solid State Chem.* **47,** 34 (1983).
6. P. E. D. Morgan and T. M. Shaw, *Mater. Res. Bull.* **18,** 539 (1983).
7. N. Yamamoto and M. O'Keeffe, *Acta Crystallogr. B* **40,** 21 (1984).
8. F. P. F. van Berkel, H. W. Zandbergen, G. C. Verschoor, and D. J. W. IJdo, *Acta Crystallogr. C* **40,** 1124 (1984).
9. N. Iyi, Z. Inoue, S. Takekawa, and S. Kimura, *J. Solid State Chem.* **52,** 66 (1984).
10. A. Kahn, T. Gbehi, J. Thery, and J.-J. Legendre, *J. Solid State Chem.* **74,** 295 (1988).
11. H. W. Zandbergen, F. C. Mijlhoff, D. J. W. IJdo, and G. van Tendeloo, *Mater. Res. Bull.* **19,** 1443 (1984).
12. N. Iyi, Z. Inoue, S. Takekawa, and S. Kimura, *J. Solid State Chem.* **60,** 41 (1985).
13. N. Iyi, Y. Bando, S. Takekawa, Y. Kitami, and S. Kimura, *J. Solid State Chem.* **64,** 220 (1986).
14. T. R. Wagner and M. O'Keeffe, *J. Solid State Chem.* **73,** 19 (1988).
15. T. Gbehi, D. Gourier, J. Thery, and D. Vivien, *J. Solid State Chem.* **83,** 340 (1989).
16. B. G. Dick and A. W. Overhauser, *Phys. Rev.* **112,** 90 (1958).
17. G. V. Lewis and C. R. A. Catlow, *J. Phys. C: Solid State Phys.* **18,** 1149 (1985).
18. C. R. A. Catlow, *Proc. Royal Soc. A* **353,** 533 (1977).
19. J.-G. Park and A. N. Cormack, *Phil. Mag. B,* in press.
20. C. R. A. Catlow, A. N. Cormack, and F. Theobald, *Acta Crystallogr. B* **40,** 195 (1984).
21. A. N. Cormack, *Solid State Ionics* **8,** 187 (1983).
22. M. J. Gillan, *Phil. Mag.* **43,** 301 (1981).
23. C. R. Peters, M. Bettman, J. W. Moore, and M. D. Glick, *Acta Crystallogr. B* **27,** 1826 (1971).
24. A. J. Lindop, C. Matthews, and D. W. Goodwin, *Acta Crystallogr. B* **31,** 2940 (1975).
25. I. D. Brown and D. Altermatt, *Acta Crystallogr. B* **41,** 244 (1985).